Search for electron liquids with non-Abelian quasiparticles

Arkadiusz Wójs

TCM Group, Cavendish Laboratory, University of Cambridge,
Cambridge CB3 0HE, United Kingdom; and
Institute of Physics, Wroclaw University of Technology,
Wyb. Wyspiańskiego 27, 50-370 Wroclaw, Poland

E-mail: `arkadiusz.wojs@pwr.wroc.pl`

Abstract. We use exact numerical diagonalization in the search of fractional quantum Hall states with non-Abelian quasiparticle statistics. For the (most promising) states in a partially filled second Landau level, the search is narrowed to the range of filling factors $7/3 < \nu_e < 8/3$. In this range, the analysis of energy spectra and correlation functions, calculated including finite width and Landau level mixing, supports the prominent non-Abelian candidates at $\nu_e = 5/2$ (paired Moore–Read "pfafian" state) and 12/5 (clustered Read–Rezayi "parafermion" state). Outside of this range, the noninteracting composite fermion model with four attached flux quanta is validated, yielding the family of quantum liquids with fractional, but Abelian statistics. The borderline $\nu_e = 7/3$ state is shown to be adiabatically connected to the Laughlin liquid, but its short-range correlations are significantly different.

1. Introduction

The incompressible quantum liquids (IQLs) [1] continue to be the subject of extensive studies ever since the famous discovery of the fractional quantum Hall (FQH) effect [2]. The IQLs are formed by two-dimensional electrons placed in a high magnetic field B which causes them to fill a particular fraction ν of one of the lowest Landau levels (LL$_n$, $n = 0$, 1, ...). The most recent storm of interest in the IQLs is motivated by the concept of "topological quantum computation" [3, 4] employing non-Abelian statistics of some of the wave functions proposed for a partially filled LL$_1$. The main idea is that the quantum information may be encoded in (topologically) different quantum states corresponding to the same spatial configuration of the non-Abelian quasiparticles (QPs) of a given underlying IQL. Transition between such different states would only be possible by a global transformation of the QP braiding, thereby making quantum information inherently protected from decoherence caused by any local processes (e.g., coupling to phonons or atomic spins). The best known candidate for a non-Abelian wave function is the "pfaffian" state proposed by Moore and Read [5, 6] and believed to describe the FQH state in a half-filled LL$_1$. Other wave functions with different complexities of braiding statistics have also been proposed [7, 8, 9, 10]. The convincing demonstration of non-Abelian statistics in a real physical system has clearly risen to the challenge of greatest importance.

The reason to search for the signatures of non-Abelian statistics in LL$_1$ is that, on the one hand, the partially filled LL$_0$ are successfully described by the composite fermion (CF) theory [11] predicting fractional but Abelian QPs and, on the other hand, that higher LLs favor ordered

electron phases. Crucial recent experiments in LL_1 include confirmation [12] of the anticipated QP charge of $e/4$ for the half-filled state at $\nu_e = 5/2$ and careful measurements [13, 14] of the minute excitation gaps. In theory, some of the most recent advances are related to the role of layer width [15] and LL mixing [16, 17] in real systems, and the nature of the QPs [18, 19].

It is quite remarkable that, despite intensive studies, connection of the FQH states in LL_1 ($\nu_e = 5/2$, $7/3$, $12/5$, or $11/5$) to the few proposed wave functions remains yet to be conclusively established. In fact, in some cases it seems only tentatively assumed for the lack of other candidates. This is an urgent problem, as the anticipation of non-Abelian statistics in nature is largely driven by the connection of some of these wave functions to the particular conformal field theories. A wealth of IQLs found in various systems (electrons or CFs at different fillings of different LLs, in layers of varied width w) also invites a more general question of possible IQLs with arbitrary LL filling ν and interaction V.

This paper is an extension of our brief communication [20]. We report here on the use of large scale exact diagonalization in the search of IQLs with non-Abelian statistics. We demonstrate that non-Abelian IQLs in LL_1 can only emerge in the narrow, particle-hole symmetric range of filling factors $7/3 < \nu_e < 8/3$. In this range, the known non-Abelian candidates at $\nu_e = 5/2$ and $12/5$ are closely examined (including such previously neglected realistic effects as finite layer width and LL mixing) and found to have favorable correlation energies. Outside of this range, the LL_1 hosts the family of Abelian ground states of noninteracting CFs each carrying four magnetic flux quanta, repeating the states known from the lowest LL. The borderline $\nu = 1/3$ ground state in LL_1 is adiabatically connected to the Laughlin state of LL_0, but it has a smaller gap and distinct short-range correlations.
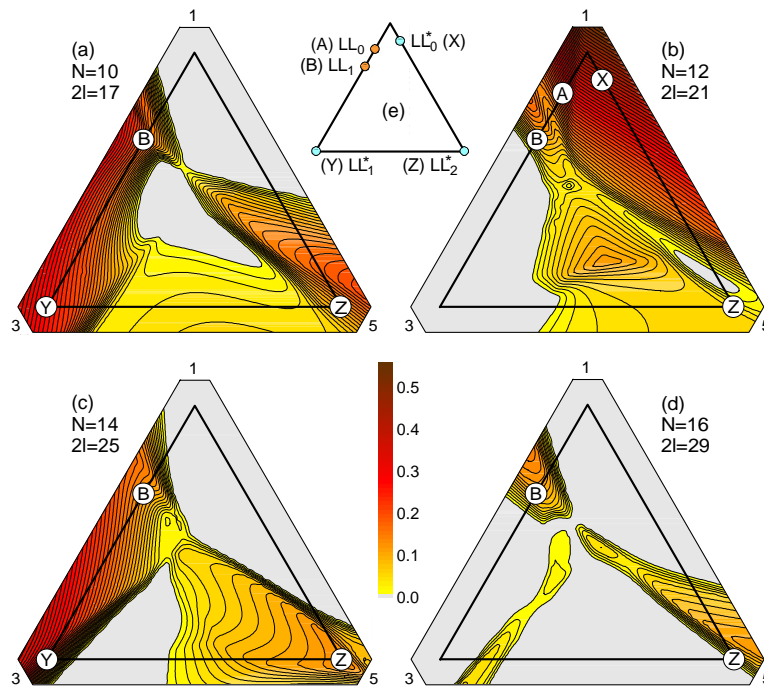
2. Model
We consider the systems of N spin-polarized fermions (electrons) on a Haldane sphere with unit radius and the magnetic monopole of strength $2Q(hc/e)$ inside [21]. In this geometry, LL_n is a shell of angular momentum $\ell = Q + n$, and different N-body wave functions at the same ν are (unlike on a torus) conveniently distinguished by a 'shift' γ between the LL degeneracy and $\nu^{-1}N$ (i.e., $2l = \nu^{-1}N - \gamma$). In contrast to the previous exact diagonalization studies we begin by searching the universality classes (ν, γ) of the gapped ground states with arbitrary interactions V rather than confining ourselves to the particular physical systems defined by n, w, etc.

It is a trivial fact that the many-body dynamics in a degenerate LL is completely determined by an interaction pseudopotential, defined [21] as the dependence of the pair energy V on the relative angular momentum $m = 1, 3, \ldots$. Less obviously, V_m induces particular correlations only through its deviation from a reference "harmonic pseudopotential" given by a straight line over the consecutive m's [22]. Hence, the low-energy spectra of V_m can be accurately reproduced by a suitable effective pseudopotential U_m with only a few appropriate coefficients.

In our calculations we have used $U = [U_1, U_3, U_5]$. Higher-order terms have been ignored, as they are essentially irrelevant for the dynamics in a liquid phase with short-range correlations. On the other hand, going beyond the (earlier used) U_1 and U_3 was needed for an improved description of the two lowest (electron or CF) LLs known to host IQL states. At the same time, it still allowed for useful graphical representation of the ground state properties in an effectively two-dimensional space of the (normalized, $\sum_m U_m = 1$) parameters U_m.

3. Maps of the gap for arbitrary interaction
Searching for the series of gapped ground states with particular filling factor ν and shift γ, we looked at various finite systems $(N, 2\ell)$. A few maps of the 'neutral' energy gap Δ for $\nu = 1/2$ and $\gamma = 3$ (i.e., $2\ell = 2N - 3$, as appropriate for the Moore–Read pfaffian state) are shown in Fig. 1. The gap Δ is defined as the energy difference from the ground state to the first excited state in the same spectrum as long as the ground state happens to be nondegenerate (i.e., has

Figure 1. Ternary contour plots of the neutral excitation gap Δ for $N = 10, 12, 14, 16$ fermions in a half-filled Landau level ($\nu = 1/2$) with shell angular momentum ℓ corresponding to the shift $\gamma = 3$ of the Moore–Read "pfaffian" wave function, interacting by model pseudopotential U_m. In each plot, three corners of the big triangles correspond to $U_m = \delta_{m,\mu}$ with $\mu = 1, 3, 5$ marked in each corner. Points relevant for the actual interactions in different electron or CF Landau levels are marked on a triangle in frame (e). Different candidate incompressible states are indicated.

zero total angular momentum, $L = 0$); otherwise Δ is set to zero. The IQL candidates are the islands of positive Δ repeating regularly in the same area of the map for different values of N. Their location on the map must be compared with the actual pseudopotentials in different LLs, as indicated in frame (e). In particular, (A) and (B) mark the appropriate positions of the electron pseudopotentials in LL_0 and LL_1 (the former dominated by V_1; the latter roughly linear between $m = 1$ and 5), and (X), (Y), and (Z) mark the same for the CFs in their effective shells LL_0^*, LL_1^*, and LL_2^*.

The appearance of a significant gap around the point (B) in all maps in Fig. 1 (i.e., for each N) confirms quite definitively the earlier expectation that the Moore–Read ground state forms for a class of pseudopotentials close to that of LL_1. It also demonstrates that its accuracy depends sensitively on the fine-tuning of the leading V_m's, achieved (for example) by adjusting the layer width w [15]. Remarkably, the maps in Fig. 1 also preclude the Moore–Read state at the half-filling of other LLs (e.g., of the second CF LL, called LL_1^*, characterized by a dominant repulsion at $m = 3$ [23]). Clearly, the microscopic origin of the FQH state observed at $\nu_e = 3/8$ [24] (in the CF picture, corresponding to $\nu = 1/2$ in LL_1^*) must be different.

Analogous maps of Δ for the Laughlin filling fractions $\nu = 1/3$ and $1/5$ are shown in Fig. 2. In (a), the universality class of the Laughlin wave function ($\nu = 1/3$ and $\gamma = 3$) is shown to cover a large part of the map, including (A) and (X), and possibly also (B) and (Z). Point (B), the most interesting for the present analysis, falls just inside the island of positive gap Δ, suggesting connection of the $\nu_e = 7/3$ FQH state to the Laughlin $\nu = 1/3$ liquid in LL_1. Point (X) is relevant for the Laughlin $\nu = 1/3$ state of the CF vacancies in LL_0^*, i.e., to the robust
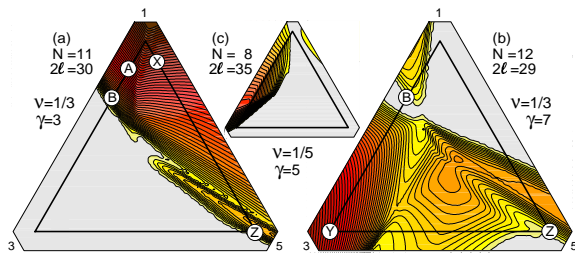
Figure 2. Similar to Fig. 1, but for Laughlin filling fractions $\nu = 1/3$ (two candidate states with $\gamma = 3$ and 7) and $\nu = 1/5$.
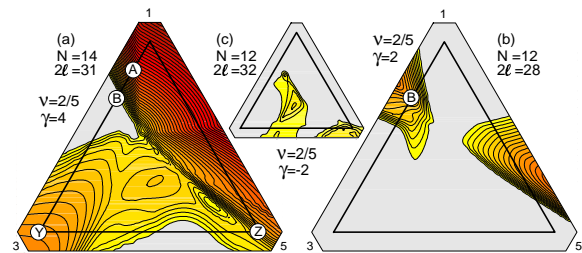

Figure 3. Similar to Fig. 1, but for the $\nu = 2/5$ states with $\gamma = 4$ (Jain), 2 (Bonderson–Slingerland), and -2 (Read–Rezayi).

Jain state at $\nu_e = 2/7$. Remarkably, the Laughlin ground state does not occur around point (Y) corresponding to the $\nu = 1/3$ filling of LL_1^*. The nature of the rather fragile FQH state observed at the corresponding fraction $\nu_e = 4/11$ [24] must therefore be different. In (b), the $\nu = 1/3$ paired (non-Laughlin) state with $\gamma = 7$, proposed earlier for both LL_1 [22] and LL_1^* [25], is tested. The gap around (Y) is quite suggestive that it may indeed describe the FQH state at $\nu_e = 4/11$ [24]. On the other hand, its relevance for LL_1 seems doubtful. In (c), any positive $U = [U_1, U_3, 0]$ yields an exact Laughlin state at $\nu = 1/5$. Our map of Δ confirms that it is true description of the FQH states in both LL_0 and LL_1 [26]. On the other hand, its relevance to the FQH effect observed in LL_1^* (i.e., at $\nu_e = 6/17$) [24] is rather unlikely.

Finally, the maps of Δ for the $\nu = 2/5$ filling have been shown in Fig. 3. In (a), the Jain series of noninteracting CF states with $\gamma = 4$ correctly represents the ground state in LL_0 (and LL_0^*). Point (B) corresponding to LL_1 lies just outside the borders of the island of $\Delta > 0$, leaving the question of relevance of the non-interacting CF picture at $\nu_e = 12/5$ open. Two other candidate ground states at $\nu = 2/5$ are the parafermion state with $\gamma = -2$ [7] and a more recently proposed state with $\gamma = 2$ [9]. Especially for the latter state, frame (b) appears suggestive of a gap emerging around (B). Clearly, the competition between these three candidate ground states in LL_1 is not convincingly resolved based on the maps of Δ alone. On the other hand, the identification of the true ground state is crucial, because the candidates with $\gamma = \pm 2$ are both non-Abelian, in contrast to the $\gamma = 4$ Jain state. More careful analysis will follow in subsequent sections.

4. Maps of the amplitudes for arbitrary interaction

Maps similar to those in Figs. 1–2 can also be used to show dependence of other parameters of the spectrum on the form of interaction. For example, in Fig. 4 we plot maps of the leading pair and triplet Haldane amplitudes for the ground states of $(\nu, \gamma) = (1/2, 3)$ and $(1/3, 3)$. The amplitudes are defined [27] as the fractions of the pairs or triplets with a given relative angular momentum m (for the pairs, $m = 1, 3, 5, \ldots$ is a measure or an average square distance; for the triplets, $m = 3$, $5, 6, \ldots$ measures an average area). These (discrete) correlation functions are particularly useful in identifying Laughlin and Moore–Read states, as they both are unique zero-energy states of simple repulsions: the former at the minimum pair angular momentum $m = 1$, the latter at the minimum triplet angular momentum $m = 3$ (hence, their corresponding amplitudes vanish exactly). The emergence and location of the islands of essentially zero amplitude in Fig. 4(c) and (d) provides additional and quite decisive support for the Laughlin $\nu = 1/3$ and Moore–Read $\nu = 1/2$ ground states (universality classes) in LL_0 and LL_1, respectively. On the other hand, other questions, such as of a Laughlin state in LL_1, remain open until the competition with other possible states (with the same ν but different γ) can be resolved.
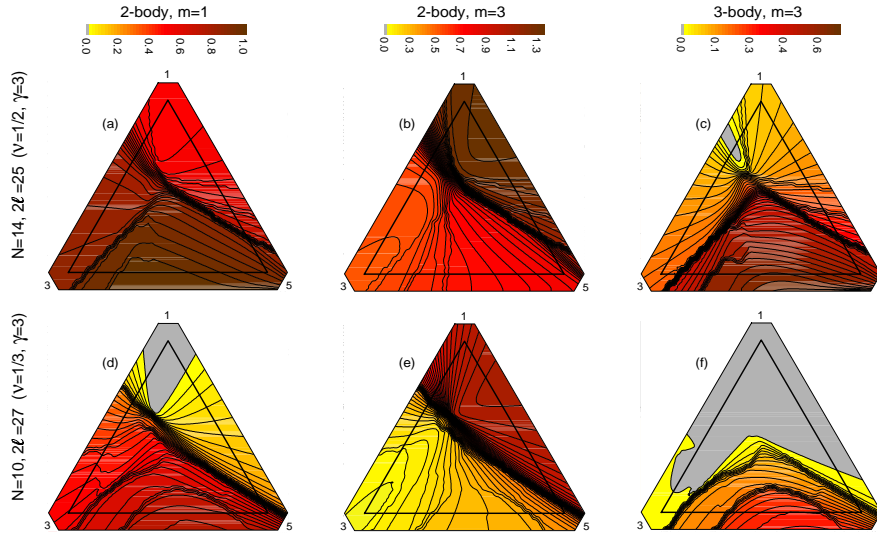
Figure 4. Ternary contour plots (similar to Fig. 1) of the pair and triplet amplitudes (labeled by the relative angular momentum m) for the universality classes of Laughlin and Moore–Read wave functions (filling factors $\nu = 1/3$ and $1/2$, respectively; shift $\gamma = 3$ in both cases).
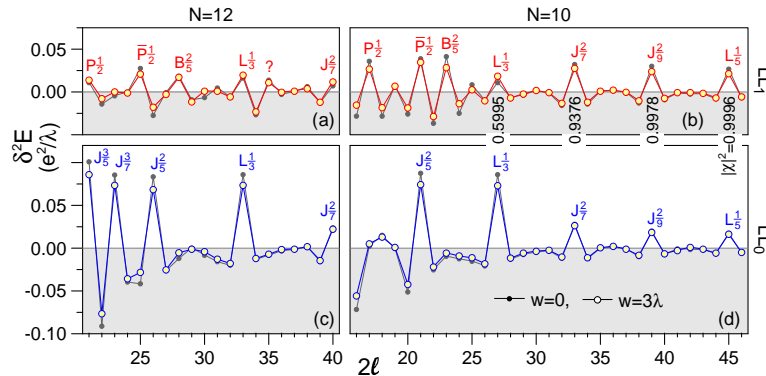
Figure 5. Symmetric second-order differences $\delta^2 E$ of the ground-state energy per particle E for $N = 10$ and 12 electrons in the lowest and second Landau level (LL_0 and LL_1), as a function of shell angular momentum ℓ, for layer widths $w = 0$ and 3λ. Candidate incompressible states are marked as '$\Phi\nu$', where $\Phi = P, \overline{P}, L, J, B$ denote Moore–Read pfaffian, anti-pfaffian, Laughlin, Jain, and Bonderson–Slingerland states. Squared overlaps $|\chi|^2$ between the states repeating in both LLs at $\nu \leq 1/3$ are indicated. λ is the magnetic length.

5. Analysis of correlation energies in LL_0 and LL_1

Guided by the maps of gaps and amplitudes we now move our focus to the FQH states in a partially filled LL_1. In Fig. 5 we seek confirmation of the IQL candidates in the downward cusps of the dependence of the ground-state correlation energy per particle E on the LL degeneracy (for a fixed number of electrons N). The correlation energy E is calculated from the total Coulomb energy $\mathcal{E}$ of N electrons in a LL shell with a given ℓ by adding the energy of attraction to the uniform charge-compensating background and dividing by N. In the calculation for finite width w of a quasi-2D electron layer, the Coulomb matrix elements were computed assuming infinite-well confinement in the perpendicular direction, i.e., for the charge-density profile of $\varrho(z) = (2/w)\cos^2(\pi z/w)$. The cusps in E are most pronounced in the plots of a symmetric
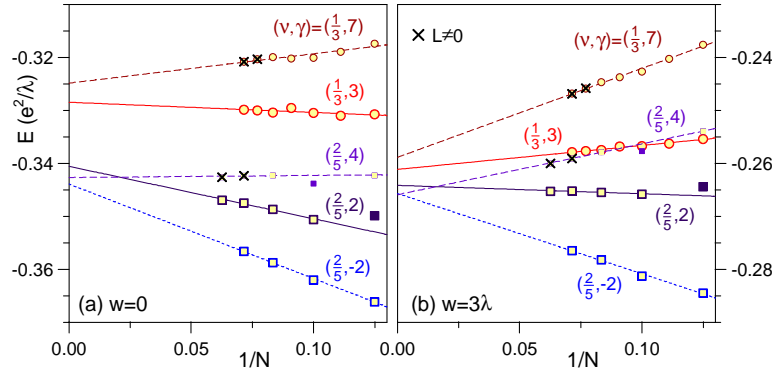
Figure 6. Size extrapolation of the ground-state correlation energies per particle E calculated for N electrons in the second Landau level (LL$_1$), for the layer widths $w = 0$ (a) and 3λ (b). Competing series of candidate incompressible ground states with filling factors $\nu = 1/3$ and $2/5$ are distinguished by their shifts γ.

difference $\delta^2 E_{2\ell} = E_{2\ell-1} + E_{2\ell+1} - 2E_{2\ell}$. For an IQL, its (positive) value gives the QP gap $\tilde{\Delta}$ (energy needed to create a pair of noninteracting QPs of total charge zero) times the number of QPs created per flux quantum.

Evidently, Fig. 5 complements the maps of Fig. 1-4 in the identification of the universality classes of particular IQLs. For example, it shows peaks in $\delta^2 E_{2\ell}$ which signal the Laughlin $\nu = 1/3$ and Moore–Read $\nu = 1/2$ IQLs in LL$_1$. But Fig. 5 also does more, by revealing the following connection between quantum statistics and the filling factor in a partially filled LL$_1$. At $\nu < 1/3$ the same Laughlin and Jain IQLs of filled shells of noninteracting CFs with four flux quanta occur in LL$_1$ and LL$_0$. The corresponding states in LL$_1$ and LL$_0$ have high overlaps (calculated by replacing the electron positions by the guiding centers) and similar QP gaps $\tilde{\Delta}$. This similarity, earlier pointed out in Ref. [26], is caused by a sufficiently high pseudopotential coefficient V_1 (forcing the avoidance of the $m = 1$ pair state) and a similar behavior of the pseudopotential al long range, $V_{m \geq 3}$, in the two lowest LLs. Importantly, this similarity validates the noninteracting CF model [11] with four flux quanta attached to each electron in LL$_1$ (in addition to LL$_0$ where its accuracy is well-known).

In contrast, at $\nu > 1/3$ the Jain sequence of noninteracting CF states in LL$_0$ is replaced in LL$_1$ by a different set of IQLs, including the Moore–Read pfaffian at $\nu = 1/2$, the anti-pfaffian (pfaffian's particle-hole conjugate) at the same $\nu = 1/2$ but with a different shift $\gamma = -1$, and a Bonderson–Slingerland $\nu = 2/5$ state with $\gamma = 2$. The breakdown of the noninteracting two-flux CF model in LL$_1$ opens, exclusively at $1/3 < \nu < 2/3$, possibility for other IQLs, including several suggested more exotic states with various non-Abelian QP statistics. The borderline $\nu = 1/3$ state, separating the Abelian from (possibly) non-Abelian states, has a moderate overlap with the Laughlin state of LL$_0$, despite falling into the same class of $\gamma = 3$.

Having narrowed the search for non-Abelian IQLs in LL$_1$ to the range of $1/3 < \nu < 2/3$, let us now try to resolve more decisively the competition between different candidate wave functions at filling factors $\nu = 1/3$ and $\nu = 2/5$ (at $\nu = 1/2$, the Moore–Read pfaffian appears to have no competition). In Fig. 6 we attempt to extrapolate to an infinite system size (to $N^{-1} \to 0$, i.e., to the planar geometry) the ground-state correlation energies per particle E. To improve convergence, the plotted energies E have been rescaled by $\sqrt{2Q\nu/N}$ so as to ensure equal units e^2/λ for each γ; here $\lambda = \sqrt{hc/eB}$ is the magnetic length). In the extrapolation for $\nu = 2/5$ we only used the open squares, discarding one state aliased with the anti-pfaffian (a finite system defined by N and 2ℓ may sometimes represent states with different combinations of ν and γ)

and one apparently suffering from the small size. When choosing the IQL ground state we also checked if a given candidate series (ν, γ) consistently has a nondegenerate (i.e., one with $L = 0$) ground state. In those cases when the particular $(N, 2\ell)$ ground state had $L \neq 0$, we crossed out the corresponding data point in Fig. 6 to mark that the series containing it is unlikely to describe an IQL in the thermodynamic limit.

For $\nu = 1/3$ Fig. 6 eliminates the (paired) $\gamma = 7$ series as a viable candidate in LL_1 (it remains plausible in LL_1^* which, however, will not be further discussed here), leaving the (universality class of the) Laughlin state as the only acceptable option. For $\nu = 2/5$, the Jain series appears to extrapolate to a competitive energy, but it no longer has $L = 0$ for the larger N, and hence should probably be discarded. The remaining two candidates both consistently have $L = 0$ and both extrapolate to nearly the same E for large N (the difference in favor of the Read–Rezayi state with $\gamma = -2$ is comparable to the error of extrapolation). In realistic conditions this near degeneracy is likely to be removed by their different susceptibilities to the LL mixing. To explore this idea, we estimated the appropriate energy correction dE by including in the diagonalization additional states involving a single cyclotron excitation [16]. Specifically, in addition to the configurations with completely filled LL_0 (with both spin-↑ and spin-↓), N polarized electrons in LL_1, and empty higher LLs, we have also included configurations with one electron promoted from either LL_0 (with either spin) or from LL_1 to the next higher LL. It should be kept in mind that inclusion of only a single cyclotron excitation is not a rigorous treatment of the LL mixing. However, it is expected to reveal a possible difference in the susceptibility of the competing states to this process. In the calculation, we have assumed the Coulomb-to-cyclotron energy ratio of $\beta \equiv (e^2/\lambda)/(\hbar\omega_c) = 1.56$, corresponding to $B = 2.6$ T. Due to a large size of the Hilbert space, the values of dE could only be calculated for $N \leq 10$. However, we found that the corrections dE are far less size-dependent than the base energies E. It is therefore justified to apply the $N = 10$ estimates of dE to the values of E extrapolated from $N \leq 16$.

The results are presented in Tab. 1. Clearly, in addition to having the lowest E, the $\gamma = -2$ parafermion state also has the largest $|dE|$, and therefore it is quite convincingly predicted to define the universality class of the $\nu = 2/5$ ground state in LL_1. This is of considerable importance because this state is the only known candidate IQL [4] whose braiding rules are sufficiently complex to allow quantum computation (unlike, e.g., the Moore–Read state).

Let us now look at the pair correlation functions of the established IQL ground states at $\nu = 1/3$ and $2/5$ in LL_1. The results calculated for the largest available systems ($N = 14$ or 16,

Table 1. Extrapolated correlation energies per particle E (in the units of e^2/λ) in several series of candidate ground states (distinguished by shifts γ) at filling factors $\nu = 1/3$ and $2/5$ in LL_1, for layer widths $w = 0$ and 3λ, calculated without LL mixing. Also, corrections dE due to LL mixing (at $B = 2.6$ T), estimated for $N = 10$ (except for $N = 8$ for $\nu = 2/5$ and $\gamma = 4$).

(ν, γ)	$(1/3, 3)$	$(1/3, 7)$	$(2/5, -2)$	$(2/5, 2)$	$(2/5, 4)$
$w = 0$:					
E	-0.3285	-0.3249	-0.3439	-0.3406	-0.3427
dE	-0.0268	-0.0218	-0.0294	-0.0239	-0.0227
$E + dE$	-0.3553	-0.3467	-0.3733	-0.3645	-0.3654
$w = 3\lambda$:					
E	-0.2611	-0.2589	-0.2657	-0.2642	-0.2659
dE	-0.0087	-0.0077	-0.0095	-0.0085	-0.0071
$E + dE$	-0.2698	-0.2666	-0.2752	-0.2727	-0.2730
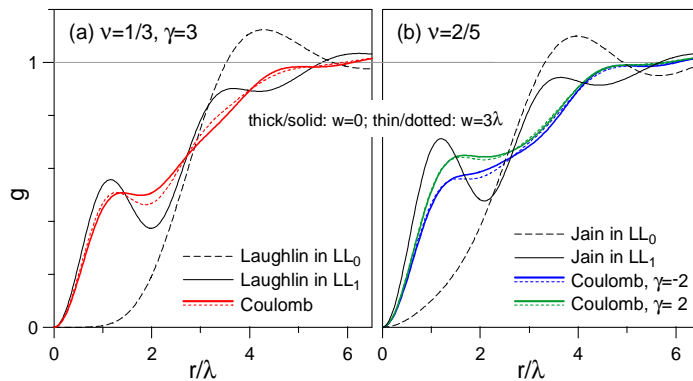
Figure 7. Pair-correlation functions of the candidate incompressible ground states at $\nu = 1/3$ (a) and 2/5 (b) in the second Landau level (LL$_1$). Coulomb ground states are compared with the exact Laughlin and approximate Jain states in LL$_0$ and LL$_1$ (constructed as the ground states of a model interaction pseudopotential with pair repulsion only at $m = 1$).
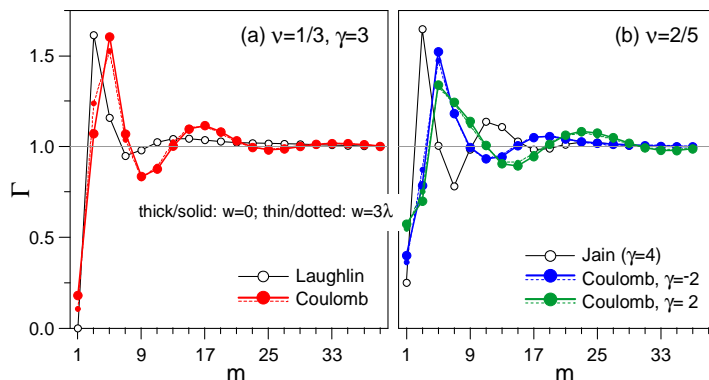
Figure 8. Renormalized pair amplitudes Γ of the same candidate states in LL$_1$ as in Fig. 7.

depending on a given state, as is clear from Fig. 6) are shown in Fig. 7. At $\nu = 1/3$, despite being adiabalitally connected to the Laughlin state (i.e., having the same $\gamma = 3$), the Coulomb ground state has significantly different short-range correlations. Specifically, the zigzag in $g(r)$ at $1 < r/\lambda < 2$ present in the exact Coulomb state in LL$_1$, caused by the particular form of the single particle wave functions and showing also in $g(r)$ for the full LL$_1$, gives way to a plateau in the case of the actual Coulomb ground state. (We should also clarify here that the Laughlin state in any LL is defined in a standard way as the zero energy state of the $m = 1$ pair repulsion, and its pair correlation function is drawn using the appropriate single-particle wave functions, e.g., of LL$_0$ or LL$_1$.) This agrees with only moderate squared overlaps of the $\nu = 1/3$ ground state in LL$_1$ with the Laughlin wave function, pointed out ourlier: 0.292 (0.501), 0.253 (0.510), 0.333 (0.549) for $N = 10$, 12, 14, for $w = 0$ (3λ). The magneto-roton band is also absent in the spectra of LL$_1$, and the low-energy states resembling Laughlin QEs and QHs are found at $2\ell = 3N - 3 \mp 1$, but they are not generally the lowest states in their spectra. A similar difference (removal of the characteristic zigzag) between the Jain state (approximated as the ground state of the $m = 1$ pair repulsion for $\gamma = 4$) and the competing Coulomb ground states with $\gamma = -2$ and 2 is also found at $\nu = 2/5$ in LL$_1$. At both filling factors dependence on w is insignificant.

Difference in short-range correlations between Laughlin and Jain states of LL$_1$ on one hand, and the $\nu = 1/3$ and 2/5 Coulomb ground states of LL$_1$ on the other, was also earlier apparent

in the leading amplitudes in Fig. 4(d,e). It is evident in the comparison of renormalized pair amplitudes Γ_m calculated for slightly larger systems (same as in Fig. 7), which have been shown in Fig. 8. Here, the coefficients Γ_m have been converted from the usual Haldane amplitudes on a sphere G_m to their planar counterparts, as described in Ref. [27]. Specifically, $\Gamma_m = 1 + (G_m - G_m^{\text{full}})/G_1^{\text{full}}$, where $G_m^{\text{full}} = (4\ell + 1 - 2m)/\ell/(2\ell + 1)$ describes a full LL.

6. Conclusion

We have carried out extensive exact diagonalization studies (including finite layer width and LL mixing) of the fractional quantum Hall states in a partially filled second Landau level (LL$_1$), searching for non-Abelian incompressible quantum liquids (IQLs). We have found the range of filling factors $1/3 < \nu < 2/3$ in LL$_1$ in which the emergence of non-Abelian statistics is possible. Inside this range, we have demonstrated that the spin-polarized ground states at $\nu = 1/2$ and $2/5$ are described by the non-Abelian "pfaffian" and "parafermion" wave functions. Outside of it, the Jain states of noninteracting CFs with four attached magnetic flux quanta repeat in both lowest LLs, thus precluding more exotic phases. The borderline $\nu = 1/3$ state is adiabatically connected to the Laughlin liquid but has a smaller gap and distinct short-range correlations.

Acknowledgment

References

[1] R. B. Laughlin, 1983 *Phys. Rev. Lett.* **50** 1395
[2] D. C. Tsui, H. L. Störmer, and A. C. Gossard, 1982 *Phys. Rev. Lett.* **48** 1559
[3] A. Yu. Kitaev, 2003 *Ann. Phys.* (N.Y.) **303** 1
[4] C. Nayak, S. H. Simon, A. Stern, M. Freedman, and S. Das Sarma, 2008 *Rev. Mod. Phys.* **80** 1083
[5] G. Moore and N. Read, 1992 *Nucl. Phys. B* **360** 362
[6] M. Greiter, X.-G. Wen, and F. Wilczek, 1991 *Phys. Rev. Lett.* **66** 3205
[7] N. Read and E. Rezayi, 1999 *Phys. Rev. B* **59** 8084
[8] G. Möller and S. H. Simon, 2008 *Phys. Rev. B* **77** 075319
[9] P. Bonderson and J. K. Slingerland, 2008 *Phys. Rev. B* **78** 125323
[10] P. Bonderson, A. Feiguin, G. Möller, and J. K. Slingerland, arXiv:0901.4965v2
[11] J. K. Jain, 1989 *Phys. Rev. Lett.* **63** 199
[12] M. Dolev, M. Heiblum, V. Umansky, Ady Stern, and D. Mahalu, 2008 *Nature* **452** 829
[13] W. Pan, J. S. Xia, H. L. Stormer, D. C. Tsui, C. Vicente, E. D. Adams, N. S. Sullivan, L. N. Pfeiffer, K. W. Baldwin, and K. W. West, 2008 *Phys. Rev. B* **77** 075307
[14] C. R. Dean, B. A. Piot, P. Hayden, S. Das Sarma, G. Gervais, L. N. Pfeiffer, and K. W. West, 2008 *Phys. Rev. Lett.* **100** 146803
[15] M. R. Peterson, Th. Jolicoeur, and S. Das Sarma, 2008 *Phys. Rev. Lett.* **101** 016807
[16] A. Wójs and J. J. Quinn, 2006 *Phys. Rev. B* **74** 235319
[17] S. H. Simon, 2008 *Phys. Rev. Lett.* **100** 116803
[18] C. Töke, N. Regnault, and J. K. Jain, 2007 *Phys. Rev. Lett.* **98** 036806
[19] B. A. Bernevig and F. D. M. Haldane, 2008 *Phys. Rev. Lett.* **100** 246802; arXiv:0810.2366
[20] A. Wójs, 2009 *Phys. Rev. B* **80** 041104(R)
[21] F. D. M. Haldane, 1983 *Phys. Rev. Lett.* **51** 605
[22] A. Wójs, 2001 *Phys. Rev. B* **63** 125312
[23] S.-Y. Lee, V. W. Scarola, and J. K. Jain, 2001 *Phys. Rev. Lett.* **87** 256803
[24] W. Pan, H. L. Störmer, D. C. Tsui, L. N. Pfeiffer, K. W. Baldwin, and K. W. West, 2003 *Phys. Rev. Lett.* **90** 016801
[25] A. Wójs, D. Wodziński, and J. J. Quinn, 2006 *Phys. Rev. B* **74** 035315
[26] N. d'Ambrumenil and A. M. Reynolds, 1988 *J. Phys. C* **21** 119
[27] A. Wójs and J. J. Quinn, 2005 *Phys. Rev. B* **71** 045324